RSC Advances

ROYAL SOCIETY OF CHEMISTRY

www.rsc.org/advances

RSC Advances

ARTICLE

Theoretical Study on the Mechanism of Oxidative-Extractive Desulfurization in Imidazolium-Based Ionic Liquid

P. Yuan,[a*] T. T. Zhang,[a] A. F .Cai,[a] C. S. Cui,[a] H. Y. Liu,[a] X. J. Bao[b*]

Received 00th January 20xx,
Accepted 00th January 20xx

DOI: 10.1039/x0xx00000x

www.rsc.org/

The aim of this paper is to theoretically investigate the mechanism of oxidative-extractive process for the removal of thiophene (TH) with the assistance of imidazolium-based ionic liquid (IL) by carrying out density functional theory calculations. The results show that IL not only plays an important role in the oxidative process by dramatically decreasing the reaction energy barriers but also exhibits an outstanding performance as an extractive agent. More importantly, we systematically explore the effect of ILs with different alkyl side chains to the imidazolium ring in both the oxidation and extraction process. It is found that with increasing the alkyl chain length from two to six carbon atoms, the energy barriers of the two elementary oxidative steps are reduced by 23% and 29%, respectively, indicating that the longer the alkyl chain, the more easily the reaction takes place. As an extractant, IL shows much stronger interactions with sulphone (SP) than TH owing to the large electronegativity and dipole moment of O atoms in SP. Moreover, natural bond orbital (NBO) analysis illustrates that cation has a greater binding force with TH or SP compared with the anion and ionic pairs, and such interaction is slightly decreased as the alkyl chain is lengthened. Our contribution is to provide a thorough explanation for the significantly enhanced oxidative-extractive desulfurization efficiency with the help of IL from the theoretical aspect, which may give a profitable guidance for the practical application.

Introduction

Nowadays, fuel desulfurization has become one of the most important oil refining processes all over the world because the presence of organosulfur compounds in petroleum not only has a negative effect on environment but also interferes with the equipment operations.[1] Hydrodesulphurization (HDS) technology is the most widely used method to produce clean gasoline/diesel with the sulfur contents even lower than 10 ppm by weight.[2] However, the conventional HDS process needs strict operating conditions, such as high temperatures, high hydrogen pressures, low space velocities and highly active catalysts, which may result in high capital investment and energy consumption. In addition, HDS may cause the unnecessary hydrogenation of olefins leading to the undesirable decrease in octane number. Therefore, many other facile and low-cost technologies for ultra-deep desulfurization have been explored, including adsorption[3] and reactive adsorption,[4] oxidation,[5-9] extraction,[10-16] and bio-desulfurization,[17]etc. Among these, the combination of oxidative and extractive desulfurization in the presence of ionic liquid (IL) is proved to be a promising method for the removal of S-containing compounds, which has attracted more and more attention and developed rapidly in recent years.[18-22] Lo et. al[23] reported that when [BMIM][BF_4] or [BMIM][PF_6] containing dibenzothiophene (DBT) was mixed carefully with H_2O_2 and acetic acid at 70 °C, the desulfurization ratios could reach to 55% and 85%, respectively, which was about 8 and 10 times higher than those obtained without the oxidation by H_2O_2. Zhao et. al[24] found that the Brønsted IL N-methyl-pyrrolidoniumtetrafluoroborate could be used as a catalyst and extractant for sulfur removal of model oil and actual diesel fuel, and the desulfurization efficiency of DBT-containing model oil could even reach to 100%, which was far superior to the simple extraction with ILs. Nejad et. al[25] compared the desulfurization efficiency of imidazolium-based ILs extraction, oxidative desulfurization (ODS) and ODS + IL-extraction using gasoline samples with different concentrations of sulfur and the result showed that the sulfur content after treatment with the combined desulfurization scheme was much lower than that after treatment with only IL or ODS, which could be reduced by > 97% for some samples. Liang et. al[26] recently reported that acetic acid-based ILs showed high activity in the oxidative desulfurization with H_2O_2 as the oxidant, and the desulfurization efficiency could reach up to 87.5%, while the sulfur removal rate was only 32.6% by single oxidation and 59.9% by simple extraction. All the recent experiment results indicate that IL plays an important role not only in the extractive process as an extractant but also in the oxidative process as a catalyst, thus the comprehensive understanding of the desulfurization mechanism in oxidative-extractive process with the assistance

[a] State Key Laboratory of Heavy Oil Processing, China University of Petroleum, Beijing 102249, China.
[b] The Key Laboratory of Catalysis, China University of Petroleum, Beijing 102249, China
*Email: yuanpei@cup.edu.cn; baoxj@cup.edu.
Electronic Supplementary Information (ESI) available: See DOI: 10.1039/x0xx00000x

of IL is critical for the development of efficient desulfurization method to produce ultra-clean fuels.

Recently, many efforts have been made to theoretically investigate the IL-extraction mechanism[27-29] and the interactions between IL and the oxidative productions of sulfur-containing compounds,[30] which have proved the much stronger interaction of IL with sulfone compounds than with thiophenic compounds. However, the theoretical study on the IL-assisted oxidative process is rarely reported.[31] More importantly, the experiment results have indicated that the structure of IL, such as the length of the alkyl side chain to the imidazolium ring, has a significant effect on the desulfurization efficiency,[26, 32] but to the best of our knowledge, such effect of IL's structure remains untouched from the theoretical perspective and the mechanism details are still ambiguous and worthy of further exploration.

In order to profoundly understand the IL structure effect and also the roles of IL on the oxidative and extractive process for the removal of thiophene (TH), herein we chose four imidazolium-based ILs with different alkyl groups to the imidazolium ring as the investigated subjects and the mechanism of oxidizing TH into sulphone (SP) by H_2O_2 without and with ILs is explored by using density functional theory (DFT) at B3LYP/6-311++G (d, p) level. It is indicated that the energy barriers of two elementary steps involved in the transformation from TH to SP were dramatically decreased with the assistance of IL, more importantly, the longer the side chain length, the more reaction energy barrier can be reduced. For the extraction process, the binding energies of whatever the cation, anion or ionic pairs with SP are much higher than those with TH owing to the large electronegativity and dipole moment of O atoms in SP. It is also found that the cation has a greater capturing ability for TH or SP compared with the anion and ionic pairs, and the interaction between the cation and TH or SP is slightly decreased with the increase of the alkyl side chain length to the imidazolium ring. Moreover, natural bond orbital (NBO) analysis was carried out to reveal the intrinsic property of interactions between ILs with SP and TH in the extraction process. Our work provides a fundamental understanding on the IL-assisted ODS process and reveals the important roles of IL in the oxidative and extractive step, which will help to develop a clean and efficient way to acquire the ultraclean fuel.

Theoretical Calculations

All stable geometries were optimized by using hybrid Becke-3-Lee-Yang-Praa exchange-correlation functional (B3LYP) method. In order to describe the molecular interaction correctly, the 6-311++G (d, p) basis set was applied as it is considered to be an available function which can provide a reliable result for IL.[31, 33-35] There are no restrictions on symmetries for the initial structures and the geometry optimization for the saddle points was occurred with all degree of freedom. In order to verify the reasonability of the optimized structures and to determine the thermal energy, the results were followed by the frequency calculations. The interaction energy is defined as the difference between the energy of IL-TH/SP ($E_{IL\text{-}TH/SP}$) and the sum of the energies of the purely IL (E_{IL}) and sulfur-containing compound ($E_{TH/SP}$).

$$\triangle E=E_{IL\text{-}TH/SP}-(E_{IL}+E_{TH/SP}) \quad (1)$$

Where $E_{IL\text{-}TH/SP}$ represents the energies of IL-TH or IL-SP, E_{IL} and $E_{TH/SP}$ is the individual energies of IL, and TH or SP; ΔE is the interaction energies between IL and TH or SP. The effects of the basis set superposition (BSSE) on the interaction energy have also been considered. All the interaction energies are corrected by BSSE calculations.

Natural bond orbital (NBO) analysis was performed to confirm the existence of the hydrogen bond. A second-order perturbation theory analysis of the FOCK matrix was carried out to evaluate the extent of electron delocalization from donors to acceptors which is reflected by the second-order perturbation stabilization energy (E(2)).[36, 37] The value of E(2) represents the ability of electrons to transfer from donor to acceptor orbitals, thus the higher the value, the stronger interaction between the donor and acceptor.

The processes of oxidizing TH to SP by H_2O_2 without or with the different imidazolium-based ILs were investigated by transition state searches, performed at the same theoretical level with the transition state (TS). All of DFT calculations were carried out with Gaussian 09 package[38] and taken electron correlation in the self-consistent Kohn-Sham for consideration. Four imidazolium-based ILs with ethyl, butyl, amyl and hexyl side alkyl chain to the imidazolium ring we chose in this calculation are named as [EMIM][PF_6], [BMIM][PF_6], [AMIM][PF_6] and [HMIM][PF_6], respectively.

Results and discussion

Geometric structure of ILs

Take the structural optimization of [BMIM][PF_6] for example, four possible configurations with [PF_6]$^-$ located at different positions around [BMIM]$^+$ are obtained as shown in Fig. S1. The optimized energies are calculated and listed in Table S1. It is obvious that the configuration (A) in Fig. S1 has the lowest energy (-316.9 kJ/mol), thus it should be the most stable structure of [BMIM][PF_6]. The optimized structures for the other three ILs were determined through the similar processing procedure (the detailed information is not shown here) and based on their optimized interaction energies (Table S1), the most stable geometries of [EMIM][PF_6], [BMIM][PF_6], [AMIM][PF_6] and [HMIM][PF_6] are given in Fig. 1.

As shown in Fig. 1, it can be found there exist six H⋯F interactions. Take [EMIM][PF_6] as an example, the H⋯F interaction distances are 2.27 (H6⋯F1), 2.24 (H2⋯F1), 2.60 (H2⋯F2), 2.11 (H2⋯F3), 2.40 (H7⋯F3) and 2.50 (H8⋯F2) Å, respectively, which are longer than the covalent bond distance of H-F and shorter than the Van Der Waals distance of H⋯F.

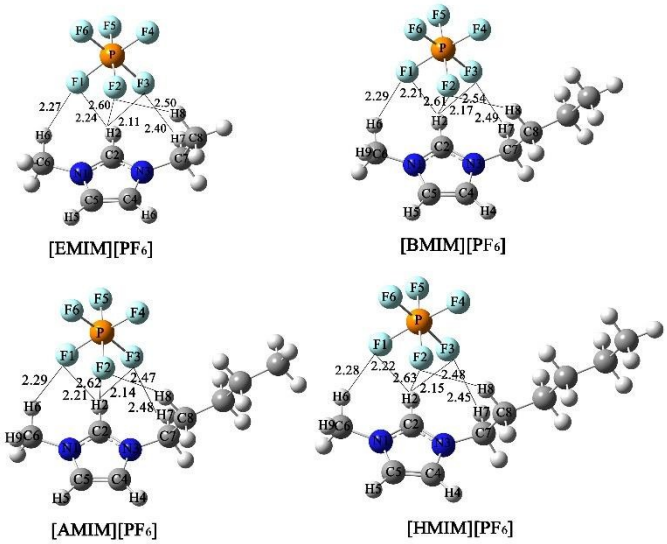

Fig. 1. The most stable geometric structures of the four ILs with different alkyl side chains to the imidazolium ring optimized at B3LYP/6-311++G (d, p) level. The distances are given in angstroms.

For the shorter distances (H2···F3, H2···F1, H6···F1), their relatively strong interactions may be ascribed to the highly positive H2 and H6 atoms due to the withdrawing electron action of the nitrogen atom around. In this system one hydrogen atom may participate in two hydrogen bonds or even three hydrogen bonds instead of one. This type of bonding is called "bifurcated bonding (three-center hydrogen bonding)" or "trifurcated hydrogen bonding (four centered hydrogen bonding).[39-41] The results show that the atom H2 in cation is involved in the formation of trifurcated hydrogen bonding, suggesting that C2-H2 plays a crucial role in the interaction between $[EMIM]^+$ and $[PF_6]^-$.

The interaction energies (ΔE) of $[EMIM][PF_6]$, $[BMIM][PF_6]$, $[AMIM][PF_6]$ and $[HMIM][PF_6]$ are calculated to be -318.8, -316.9, -316.2 and -311.2 kJ/mol, respectively. It is noted that the absolute value of ΔE is decreased with the increase of alkyl chain length to imidazolium ring, in other words, the stability is slightly decreased as the alkyl chain lengthens. According to the NBO results, the sum of the NBO positive charges on H6, H2, H7 and H8 atoms for the selected four ILs is 0.945 for $[EMIM][PF_6]$, 0.937 for $[BMIM][PF_6]$, 0.932 for $[AMIM][PF_6]$ and 0.931 for $[HMIM][PF_6]$, while the sum of NBO negative charges on F1, F2 and F3 atoms is -1.915, -1.913, -1.914 and -1.913, respectively, indicating the electron density is influenced by the alkyl side chain. NBO results further reveal the slightly decreased interaction between the cation and anion species as the increase of alkyl chain length, in good agreement with the interaction energy calculations. Three-dimensional plots of the electrostatic potential surface for the four ILs are shown in Fig. S2. The red color represents the negative charge region and the blue color expresses the positive charge region and the deeper the colour, the greater the charge density. Despite of the different alkyl substituents to imidazolium ring, the charge density distribution is similar to each other. But it should be noted that along with the increase of the alkyl side chain length, the charge distribution becomes more uniform and the positive charge on the methyl to imidazolium ring is slightly decreased.

The oxidation mechanism of TH by H_2O_2 without and with IL

The oxidative reaction formula of TH to SP by H_2O_2 in the absence of ILs is given in Fig. 2A, which reaction actually experiences two elementary steps from TH (R1) to THO (P1) then finally to SP (P2) via two immediate processes (IM1 and IM2) and two transition states (TS1 and TS2) as shown in Fig. 2B. Firstly, when H_2O_2 approaches to TH, the O1 atom in H_2O_2 forms chalcogen bond[42, 43]with S atom in TH. Chalcogen bond is defined as a specific intermolecular interaction involving S atom as an electron donor and its strength and directionality can be comparable to hydrogen bond. Because of the attractive interaction between S and O1 atom, the distance between S···O1 decreases from 2.68 to 2.09 then to 2.04 Å while the distance between O1 and O2 increases from 1.53 to 1.97 then to 2.01 Å, as a result P1 is formed. After that, O atom from another H_2O_2 molecule continues to attack S atom of P1 following the similar process as described above and finally SP is produced.

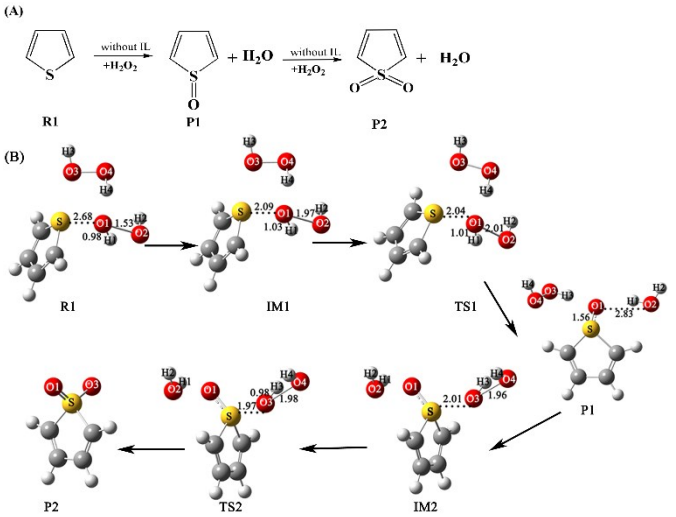

Fig. 2. (A) The reaction formula of oxidizing TH to SP by H_2O_2; (B) Mechanism of the oxidation process from TH to SP with H_2O_2. The distances are given in angstroms.

The calculated energy profiles of the oxidation process are shown in Fig. 3 and the relevant energies are given in Table1. Obviously, the energies in the first intermediate state (IM1) and the first transition state (TS1) are higher than the reactant by 48.7 and 385.5 kJ/mol, respectively, and the energy barrier of the first oxidation step is as high as 336.8 kJ/mol (ΔE_{TS1}-ΔE_{IM1}). In the second oxidation step, another H_2O_2 molecule approaches to sulfoxide (P1) to form chalcogen bond with S atom and the intermediate state (IM2) is lower than P1 by 125.8 kJ/mol, indicating the sulfoxide is not stable and quite easily to be attacked by H_2O_2. The energy barrier of the second step is calculated to be 285.3 kJ/mol. It is noted that the two elementary steps involve high energy barriers, implying that the oxidization reaction of TH to SP by H_2O_2 needs very high energy and cannot occur under room temperature conditions without the assistance of a catalyst.

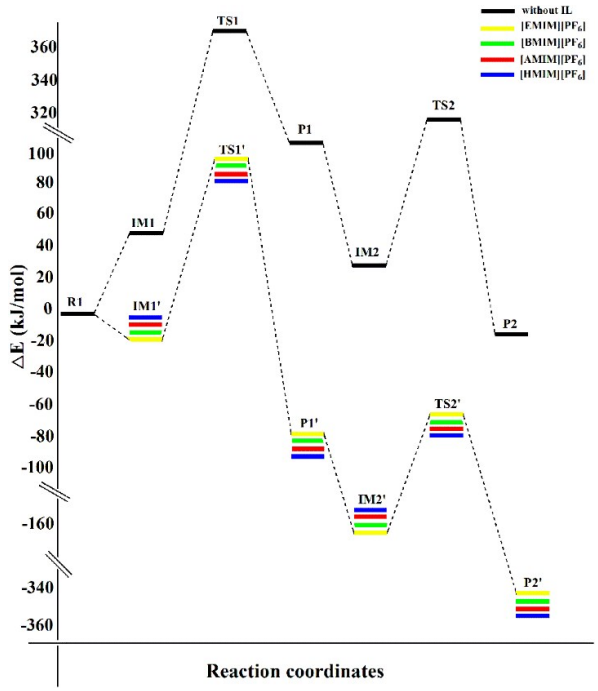

Fig. 3. Energy profiles for the oxidation reaction from TH to SP by H_2O_2 without and with the assistance of ILs with different alkyl side chains to the imidazolium ring calculated at B3LYP/6-311++G (d, p) level.

Table. 1. Calculated energy in each oxidative step from TH to SP by H_2O_2 without and with the assistance of ILs with different alkyl side chains to the imidazolium ring at B3LYP/6-311++G (d, p) level. (The unit of the energy is kJ/mol).

	IM1	TS1	P1	IM2	TS2	P2
Without ILs	48.7	385.5	151.9	26.1	311.4	-35.8
[EMIM][PF_6]	-14.7	100.7	-83.0	-168.1	-59.1	-341.8
[BMIM][PF_6]	-11.4	99.4	-88.2	-168.3	-72.0	-354.2
[AMIM][PF_6]	-5.6	92.5	-89.2	-164.5	-77.5	-358.0
[HMIM][PF_6]	-2.0	87.3	-90.2	-163.8	-86.8	-363.4

When IL is added to the oxidation process, the situation is changed noticeably. In order to investigate the effect of imidazolium-based ILs with different alkyl side chains on the oxidation reaction, we simulated the above process under the presence of ILs. Firstly, the complex structures between the ionic pairs and H_2O_2 are optimized, which is the initial and essential step to calculate the following detailed reaction procedure, and the four possible initial structures of [EMIM][PF_6] with H_2O_2 are given in Fig. S3. Based on the O-O bond length in H_2O_2, position 3 is chosen as the initial structure because the activation of O-O bond is most efficient in it. Take [EMIM][PF_6] with H_2O_2 as an example, the possible pathway of the oxidation from TH to SP is calculated as shown in Fig. 4 and the oxidative transition states for the other three ILs are given in Fig. S4. The pathway involves a mechanism similar to that described without IL (Fig. 2B), which also experiences two elementary steps: TH is firstly oxidized to THO and subsequently to SP but

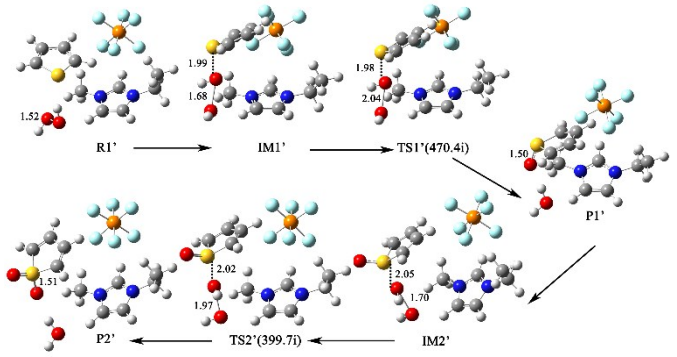

Fig. 4. Mechanism of the oxidation process from TH to SP by H_2O_2 with the assistance of [EMIM][PF_6]. The distances are given in angstroms. The values in parentheses denote the imaginary frequencies in the transition states.

the energy in each step and the energy barriers are significantly different. Firstly, the O atom of H_2O_2 in reactant 1 (R1') changes its position to move close to S atom of TH in intermediate 1 (IM1') and the O atom keeps to approach to S atom to form the chalcogen bond (O···S) in TS1'. In the first step of the oxidation process, the length of O-O bond changes from 1.52 (in R1') to 1.68 Å (in IM1') and then prolongs to 2.04 Å (in TS1'). It should be noted that the TS1' has a unique imaginary frequency at -470.4 cm^{-1}, corresponding to the stretching vibration of O-O bond, illustrating the breakage of O-O bond due to the relatively strong attraction between the O atom and S atom.[31] The formation of chalcogen bond, the increase of O-O bond length and the imaginary frequency all indicate the occurrence of the reaction and the reasonable oxidative mechanism with the assistance of IL. The electrophilic O atom in H_2O_2 interacts with the electron-rich S atom via charge attraction to produce THO as product P1'. Subsequently, a second H_2O_2 molecule is introduced into the system to form the intermediate product IM2', in which the O-O bond is activated by IL and the bond length is elongated from 1.52 to 1.70 (IM2') then to 1.97 Å (TS2') owing to the attraction between O and S atom. For TS2', it also has a unique imaginary frequency at -399.7 cm^{-1}, belonging to the stretching vibration of O-O bond, indicating the cleavage of O-O bond.

According to the energy statistics in each step (Figure 3 and Table 1), it is surprising to find that the energy barriers of two oxidation steps in the presence of [EMIM][PF_6] are significantly decreased compared with those from the process without IL, changing from 336.8 (ΔE_{TS1}-ΔE_{IM1}) and 285.3 kJ/mol (ΔE_{TS2}-ΔE_{IM2}) to 115.4 ($\Delta E_{TS1'}$-$\Delta E_{IM1'}$) and 109.0 kJ/mol ($\Delta E_{TS2'}$-$\Delta E_{IM2'}$), respectively. The result indicates that [EMIM][PF_6] plays important roles on the activation of H_2O_2 and TH and also on the stabilization of all species involved in the reaction, especially for the transition states. The other three ILs with different alkyl groups to imidazolium ring show the similar effect on the oxidation process of TH to SP by H_2O_2 but the reaction energy barriers are different. As shown in Table 1, the energy barriers of the two oxidation steps are 110.8 and 96.3 kJ/mol for [BMIM][PF_6], 98.1 and 87.0 kJ/mol for [AMIM][PF_6], 89.3 and 77.0 kJ/mol for [HMIM][PF_6], respectively. Thus the oxidation reaction can occur more easily with the assistance of IL and more importantly, the energy barriers are decreased with the

increase of alkyl side chain length. From the above analysis, such oxidative process is occurred between S atom of TH and O atom of H_2O_2, thus the electron density on these two atoms is a predominant factor to determine this reaction. The NBO result shows that the charge on S atom is influenced by the structure of IL and with the increase of the alkyl side chain from ethyl to butyl, amyl and hexyl, the number of the charge on S atom increases from 0.462 to 0.479, 0.483, and 0.485. While the side chain length to imidazolium ring of IL has little effect on the charge of O atom in H_2O_2. Therefore, the reaction is more likely to occur on S atom with higher electron density and accordingly, the lower reaction energy barrier is needed with the help of [HMIM][PF_6].

Extraction mechanism

It has been documented that the desulfurization efficiency by only using IL as an extractant is rather low (only 10-30%)[23], but when combined with the oxidation process, the efficiency will be significantly improved[23-26]. In order to deeply understand the extraction mechanism on IL, we further carefully investigated the interaction of cation moiety, anion moiety and entire ionic pairs with TH and SP, respectively, and all the interaction structures were optimized at B3LYP/6-311++G (d, p) level as shown in Fig. 5.

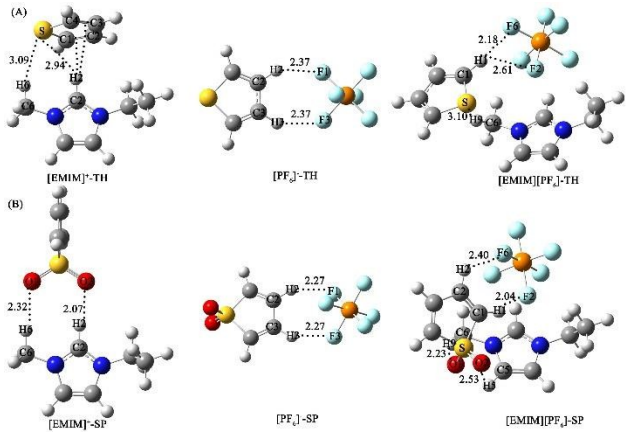

Fig. 5. Interactive geometries of (A) [EMIM]$^+$-TH, [PF_6]$^-$-TH and [EMIM][PF_6]-TH; (B) [EMIM]$^+$-SP, [PF_6]$^-$-SP and [EMIM][PF_6]-SP optimized at B3LYP/6-311++G (d, p) level.

It can be seen that the interaction between [EMIM]$^+$ and TH depends on two kinds of forces: the C6-H6 and C2-H2···S chalcogen bonds with the bond length of 3.09 and 2.94 Å and C2-H2 with C1=C2 and C3=C4 through σ-π interaction (Fig. 5A). For [PF_6]$^-$-TH complex, the H···F hydrogen bonds (H2···F1 and H3···F3) with the bond length of 2.37 Å are the main binding force. When [EMIM][PF_6] as an entirety to interact with TH, the situation is quite different from the case in the cation and anion moiety, probably due to the steric hindrance effect. The interaction is mainly through H···F hydrogen bonds, H1···F6 and H1···F2 (2.18 and 2.61 Å), and C6-H9···S chalcogen bond (3.10 Å). After the oxidation of TH to SP, the interaction between cation and SP is through C-H···O hydrogen bonds instead of C-H···S chalcogen bonds with the much shorter bond lengths of 2.32 and 2.07 Å (O1···H6 and O2···H2), respectively, implying the much stronger interaction in [EMIM]$^+$-SP than in [EMIM]$^+$-TH. For [PF_6]$^-$-SP complex, the interaction is also through the hydrogen bond between H and F atoms, but the bond length is reduced from 2.37 to 2.27 Å, indicating the interaction is strengthened after the oxidation reaction from TH to SP. The hydrogen bonds of C6-H9···O1, C5-H5···O1 (2.23 and 2.53 Å) and C2-H2···F6, C1-H1···F2 (2.40 and 2.04 Å) are the dominant interactions between the ionic pair [EMIM][PF_6] and SP. It is noted that all the interaction bond lengths in whatever cation-SP, anion-SP or ILs-SP become shorter compared with those observed in the interaction with TH, revealing the stronger capturing force for SP than for TH, which is in good accordance with the experimental results[23-26] and also consists with our calculated binding energies in Table 2.

Table 2. Binding energies of cation, anion and ionic pairs with TH and SP calculated at B3LYP/6-311++G (d, p) level corrected by BSSE calculations.

	With TH (kJ/mol)	With SP (kJ/mol)
[EMIM]$^+$	-16.2	-58.7
[BMIM]$^+$	-15.2	-56.9
[AMIM]$^+$	-15.0	-56.8
[HMIM]$^+$	-14.9	-56.6
[PF_6]$^-$	-8.1	-50.7
[EMIM][PF_6]	-7.7	-31.4
[BMIM][PF_6]	-9.6	-32.5
[AMIM][PF_6]	-9.9	-32.9
[HMIM][PF_6]	-10.3	-33.1

It can be found that the binding energies of [EMIM]$^+$, [PF_6]$^-$ and [EMIM][PF_6] with TH/SP are calculated to be -16.2/-58.7, -8.1/-50.7 and -7.7/-31.4 kJ/mol (Table 2), respectively, indicating the much greater capturing ability for SP than that for TH. Such increased interaction is attributed to the larger electronegativity and dipole moment of O atoms in SP than that of H atoms in TH. It is worth noting that the cation has higher binding energy with TH or SP compared with the anion and ionic pairs, probably due to the more or stronger interactions between cation and TH/SP. The existence of the steric hindrance in ionic pairs-TH/SP results in the weakening or disappearance of the interaction bonds and thereby the lower binding energy is obtained. Noticeably, the alkyl side chain length to the imidazolium ring also has an influence on the binding energies between cation or ionic pairs with TH or SP. The interactions of cation-TH/SP are slightly decreased with the increase of the alkyl side chain length from two to six carbon atoms, while for ionic pairs-TH/SP, the orderliness is opposite, that is to say the interaction is slightly increased as the alkyl chain is lengthened. The reason should be better explained by combining the NBO analysis which will be discussed later. Overall, based on the optimized interaction structures (Fig. 5)

and the calculated binding energies (Table 2), the reason why the extraction efficiency of IL for SP is much higher than that for TH is clear.

The NBO method can provide information about the interactions in both occupied and virtual orbital spaces which facilitates the analysis on the intermolecular interactions. The representative donor-acceptor orbitals of cation-TH/SP, anion-TH/SP, ionic pairs-TH/SP and their E(2) values are listed in Table 3. Again take [EMIM][PF_6] as an example, for the complex of [EMIM]$^+$-TH, the interaction is concentrated on the C1=C2 and C3=C4 with C2-H2, and S atom with C2-H2 and C6-H6, which is in accordance with the interactive bonds shown in Fig. 5A. Based on the electron donor-acceptor interaction and E(2) values, it can be seen that [EMIM]$^+$ is the electron acceptors and TH is the electron donors, and the interactions are mainly through the C-H σ*-bond in [EMIM]$^+$ with the π-bond on the TH ring and the lone pair electrons of S atom (LP(S)). For [PF_6]$^-$-TH, [PF_6]$^-$ as electron donors provides electrons to TH and the value of E(2) is 4.8 kJ/mol, corresponding to F⋯C-H hydrogen bond as indicated in Fig. 5. For the interaction between entire ionic pairs and TH, the primary bindings are located at F6 to C1-H1 and S to C6-H9 with E(2) values of 6.0 and 0.6 kJ/mol (Table 3), respectively. The interaction between S and ionic pairs is relatively weak and can be neglected, thus therein TH is the electron acceptors and [EMIM][PF_6] is the electron donors. When TH is oxidized to SP, the main interactions for [EMIM]$^+$-SP are changed to the lone pair electrons of O1 and O2 atoms (as electron donor) with the σ* orbitals of C6-H6 and C2-H2 (as electron acceptor) and the corresponding E(2) values are 12.5 and 34.0 kJ/mol, respectively, which are much larger than those between [EMIM]$^+$ and TH, further verifying the greatly improved extraction efficiency after oxidation. For [PF_6]$^-$-SP, the main interactions are also hydrogen bonds between F atoms and C-H with an increased E(2) values of 7.3 kJ/mol. The interactions between [EMIM][PF_6] and SP are primarily through O1 with C6-H9 and F2 with C1-H1 and the corresponding E(2) values are 6.4 and 12.2 kJ/mol, also showing the much stronger binding force than [EMIM][PF_6]-TH. For the other ILs with different alkyl side chains, the main binding interactions are similar as [EMIM][PF_6]-TH/SP, but the order of the interaction strength between the cation and TH/SP is in direct contradiction to that between ionic pairs and TH/SP. It is found that as increasing the alkyl side chain length, the values of E(2) for cation-TH/SP are decreased but those for ionic pairs-TH/SP are increased, which is consistent with the observation of the calculated binding energies in Table 2.

From the electron donor-acceptor orbital energies (Table 3), it is clear that the cations act as the electron acceptor, while ionic pairs behave as the electron donor when interacting with TH or SP.Because the straight-chain paraffin has the electron donating property which will provide electrons to the imidazolium ring, thus when the alkyl side chain length is increased, the ability of the cations to accept electrons is decreased. Likewise, the ionic pairs as the electron donor will enhance their donating electrons ability with increasing the alkyl chain length. This is the reason why the cations and ionic pairs have the opposite rules for the interaction with TH and SP but on the whole, the cation plays the predominant role in the extraction process and the extraction efficiency is significantly enhanced after the oxidation of TH to SP.

Table. 3. The electron donor-acceptor interactions and the corresponding E(2) (kJ/mol) of cation-TH, anion-TH, ionic pairs-TH and cation-SP, anion-SP, ionic pairs-SP calculated at B3LYP/6-311++G (d, p) level.

	Donor	Acceptor	E(2)/(kJ/mol)	Donor	Acceptor	E(2)/(kJ/mol)
[EMIM]$^+$-TH	π(C3=C4)	σ*(C2-H2)	3.5	LP(S)	σ*(C6-H6)	5.7
	π(C1=C2)	σ*(C2-H2)	4.9	LP(S)	σ*(C2-H2)	2.2
[BMIM]$^+$-TH	π(C3=C4)	σ*(C2-H2)	2.9	LP(S)	σ*(C6-H6)	5.4
	π(C1=C2)	σ*(C2-H2)	4.5	LP(S)	σ*(C2-H2)	1.8
[AMIM]$^+$-TH	π(C3=C4)	σ*(C2-H2)	1.6	LP(S)	σ*(C6-H6)	5.1
	π(C1=C2)	σ*(C2-H2)	4.3	LP(S)	σ*(C2-H2)	1.6
[HMIM]$^+$-TH	π(C3=C4)	σ*(C2-H2)	1.5	LP(S)	σ*(C6-H6)	5.1
	π(C1=C2)	σ*(C2-H2)	4.2	LP(S)	σ*(C2-H2)	1.7
[PF_6]$^-$-TH	LP(F1)	σ*(C2-H2)	4.8	LP(F3)	σ*(C3-H3)	4.8
[EMIM][PF_6]-TH	LP(F6)	σ*(C1-H1)	6.0	LP(S)	σ*(C6-H9)	0.6
[BMIM][PF_6]-TH	LP(F6)	σ*(C1-H1)	6.4	LP(S)	σ*(C6-H9)	0.8
[AMIM][PF_6]-TH	LP(F6)	σ*(C1-H1)	7.6	LP(S)	σ*(C6-H9)	0.5
[HMIM][PF_6]-TH	LP(F6)	σ*(C1-H1)	8.9	LP(S)	σ*(C6-H9)	0.4
[EMIM]$^+$-SP	LP(O1)	σ*(C6-H6)	12.5	LP(O2)	σ*(C2-H2)	34.0
[BMIM]$^+$-SP	LP(O1)	σ*(C6-H6)	11.6	LP(O2)	σ*(C2-H2)	33.4
[AMIM]$^+$-SP	LP(O1)	σ*(C6-H6)	11.2	LP(O2)	σ*(C2-H2)	33.2
[HMIM]$^+$-SP	LP(O1)	σ*(C6-H6)	10.7	LP(O2)	σ*(C2-H2)	32.4
[PF_6]$^-$-SP	LP(F1)	σ*(C2–H2)	7.3	LP(F3)	σ*(C3-H3)	7.3
[EMIM][PF_6]-SP	LP(O1)	σ*(C6-H9)	6.4	LP(F2)	σ*(C1-H1)	12.2
[BMIM][PF_6]-SP	LP(O1)	σ*(C6-H9)	7.9	LP(F2)	σ*(C1-H1)	13.8
[AMIM][PF_6]-SP	LP(O1)	σ*(C6-H9)	8.5	LP(F2)	σ*(C1-H1)	14.5
[HMIM][PF_6]-SP	LP(O1)	σ*(C6-H9)	9.0	LP(F2)	σ*(C1-H1)	14.6

"LP" for 1-centervalence lone pair

Fig. 6 illustrates the dominating donor-acceptor orbital interactions between the cation, anion and ionic pairs of [EMIM][PF_6] with TH and SP. The intermolecular orbital geometry shows that the primary orbital interaction of [EMIM]$^+$-TH is π(C1=C2)

→σ*(C2-H2), meaning that the electrons transfer from π orbital of C1=C2 in TH ring to the σ anti-bond orbital of C2-H2. Similarly, $[PF_6]^-$-TH has the main electron transfer from lone pair electron of F1 to the σ anti-bond orbital of C2-H2 in TH and [EMIM][PF_6]-TH shows the interaction between LP(F6) and σ*(C1-H1). While for the interaction between IL with SP, the dominant electron donor-acceptor orbital interactions are LP(O2)→σ*(C2-H2) for $[EMIM]^+$-SP, LP(F3) → σ*(C3-H3) for $[PF_6]^-$-TH and LP(F2) → σ*(C1-H1) for [EMIM][PF_6]-SP, respectively, indicating the main change is occurred on the interaction of cation with SP, which has the electron transfer from the lone pair electrons of O2 to the σ anti-bond orbital of C2-H2. It's worth mentioning that a d^2sp^3 hybridization orbital of P atom in $[PF_6]^-$ is formed, so there exist six completely identical hybridized orbitals. When the lone pair electrons of F interact with the σ anti-bonding orbital of C-H in TH, the values of E(2) are same with each other. After TH is oxidized to SP, the conjugation effects of thiophene ring is changed by the electron withdrawing atom O, as a result, the positive electron density of H atoms is increased, and the interaction between H···F in $[PF_6]^-$-SP complex are stronger than that in $[PF_6]^-$-TH. The NBO analysis is in good agreement with the results obtained from the interactive structures (Fig. 5) and binding energies (Table 2), which gives a new insight in the intermolecular interaction and also provides a persuasively interpretation for the improved sulfur removal efficiency in the IL-assisted ODS process.

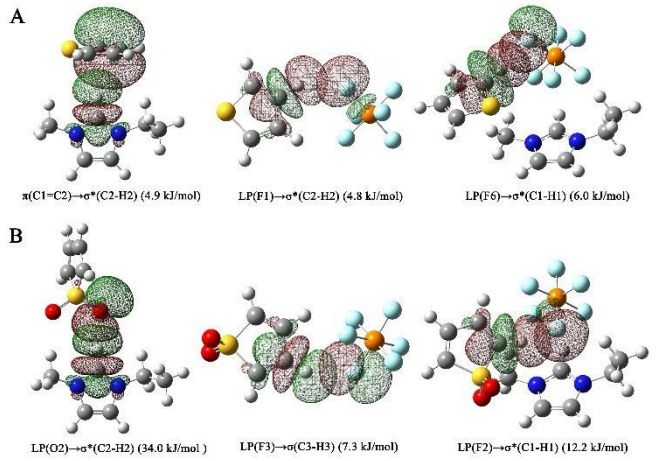

Fig. 6. The primary donor-acceptor interactions of (A): $[EMIM]^+$-TH, $[PF_6]^-$-TH and [EMIM][PF_6]-TH; B: $[EMIM]^+$-SP, $[PF_6]^-$-SP and [EMIM][PF_6]-SP calculated at B3LYP/6-311++G (d, p) level.

Conclusions

A systematically theoretical study has been performed by using density functional theory to comprehensively explore the mechanism of IL-assisted oxidative-extractive desulfurization. In the oxidation process, the energy barriers of the two elementary steps are both decreased significantly with the help of IL, in which IL acts as a catalyst to activate both thiophene and H_2O_2, making the oxidative reaction easier to take place. Such reaction energy barriers are further decreased as increasing the alkyl side chain length to the imidazolium ring of IL. In the extraction process, whatever the cation, anion or entire ionic pairs exhibit stronger interactions with SP than those with TH, attributing to the larger electronegativity and dipole moment of O atoms in SP, and this is the reason why the extractive efficiency can be greatly enhanced after the oxidation. Moreover, according to the NBO analysis, cation plays the dominant role in the capture of S-containing compounds and the interaction of the cation with TH or SP is slightly decreased with the increase of the alkyl side chain length. Our work is favourable to deeply understand the roles of IL in the oxidative-extractive desulfurization process and provides a theoretical basis for the future application.

Acknowledgements

This work was financially supported by the National Natural Science Foundation of China (Grant 21106182, 21576290) and the research fund for public welfare project (Grant 201410015).

References

1. V. C. Srivastava, *RSC. Adv.*, 2012, **2**, 759-783.
2. M. Gupta, J. He, T. Nguyen, F. Petzold, D. Fonseca, J. B. Jasinskiand M. K. Sunkara, *Appl. Catal. B*, 2016, **180**, 246-254.
3. Y. Xia, Y. Li, Y. Gu, T. Jin, Q. Yang, J. Hu, H. Liu and H. Wang, *Fuel*, 2016, **170**, 100-106.
4. R. Ullah, Z. Zhang, P. Bai, P. Wu, D. Hang, U. J. Etim and Z. Yan, *Ind. Eng. Chem. Res.* , 2016, **55**, 3751-3758.
5. H. F. M. Zaid, F. K. Chong and M. I. A. Mutalib, *Fuel*, 2015, **156**, 54-62.
6. F. L. Yu, C. Y. Liu, P. H. Xie, B. Yuan, C. X. Xie and S. T. Yu, *RSC. Adv.*, 2015, **6**, 85540-85546.
7. X. Chen, H. Guo, A. A. Abdeltawab, Y. Guan, S. S. Al-Deyab, G. Yu and L. Yu, *Energy Fuels*, 2015, **29**, 2998-3003.
8. Y. Nie, Y. Dong, L. Bai, H. Dong and X. Zhang, *Fuel*, 2013, **103**, 997-1002.
9. A. Akbari, M. Omidkhah and J. T. Darian, *Ultrason. Sonochem.*, 2015, **23**, 231-237.
10. A. Ramalingam and A. Balaji, *J. Mol. Liq.*, 2015, **212**, 372-381.
11. S. A. Dharaskar, K. L. Wasewar, M. N. Varma and D. Z. Shende, *Sep. Purif. Technol.*, 2015, **155**, 101-109.
12. O. U. Ahmed, F. S. Mjalli, A. M. Gujarathi, T. Al-Wahaibi, Y. Al-Wahaibi and I. M. Ai-Nashef, *Fluid Phase Equilib.*, 2015, **401**, 102-109.
13. O. U. Ahmed, F. S. Mjalli, T. Al-Wahaibi, Y. Al-Wahaibi and I. M. AlNashef, *Ind. Eng. Chem. Res.* , 2015, **54**, 6540-6550.
14. C. Li, D. Li, S. Zou, Z. Li, J. Yin, A. Wang, Y. Cui, Z. Yao and Q. Zhao, *Green Chem.*, 2013, **15**, 2793-2799.
15. F. Yu, C. Liu, B. Yuan, P. Xie, C. Xie and S. Yu, *Fuel*, 2016, **177**, 39-45.
16. R. Abro, A. A. Abdeltawab, S. S. Al-Deyab, G. Yu, A. B. Qazi, S. Gao and X. Chen, *RSC. Adv.*, 2014, **4**, 35302-35317.
17. S. Chaiprapat, B. Charnnok, D. Kantachote and S. Sung, *Bloresour. Technol.*, 2015, **179**, 429-435.
18. B. Jiang, H. Yang, L. Zhang, R. Zhang, Y. Sun and Y. Huang, *Chem. Eng. J.*, 2016, **283**, 89-96.

19. J.-j. Li, F. Zhou, X.-d. Tang, T. Hu and J. Cheng, *RSC. Adv.*, 2016, **6**, 4803-4809.
20. K. Liu, Z. Yao, H. N. Miras and Y.-F. Song, *ChemCatChem.*, 2015, **7**, 3903-3910.
21. A. W. Bhutto, R. Abro, S. Gao, T. Abbas, X. Chen and G. Yu, *J. Taiwan. Inst. Chem. E.*, 2016, **62**, 84-97.
22. H. Zhao and G. A. Baker, *Front. Chem. Sci. Eng.*, 2015, **9**, 262-279.
23. W. H. Lo, H. Y. Yang and G. T. Wei, *Green Chem.*, 2003, **5**, 639-642.
24. D. Zhao, J. Wang and E. Zhou, *Green Chem.*, 2007, **9**, 1219-1222.
25. N. F. Nejad, E. Shams and M. K. Amini, *Pet. Sci. Technol.*, 2014, **32**, 1537-1544.
26. W. Liang, S. Zhang, H. Li and G. Zhang, *Fuel Process. Technol.*, 2013, **109**, 27-31.
27. H. Li, Y. Chang, W. Zhu, W. Jiang, M. Zhang, J. Xia, S. Yin and H. Li, *J. Phys. Chem. B*, 2015, **119**, 5995-6009.
28. H. Li, W. Zhu, Y. Chang, W. Jiang, M. Zhang, S. Yin, J. Xia and H. Li, *J. Mol. Graphics Modell.*, 2015, **59**, 40-49.
29. A. Ramalingam and J. Jewaratnam, *Asia-Pac. J. Chem. Eng.*, 2015, **10**, 904-922.
30. P. Gu, R. Lu, D. Liu, Y. Lu and S. Wang, *PCCP.*, 2014, **16**, 10531-10538.
31. H. Xu, Z. Hau, D. Zhang and C. Liu, *J. Mol. Catal. A: Chem.*, 2015, **398**, 297-303.
32. T. Wang, D. S. Zhao, Z. M. Sun, F. T. Li, Y. Q. Song and C. G. Kou, *Pet. Sci. Technol.*, 2012, **30**, 385-392.
33. R. Anantharaj and T. Banerjee, *AIChE J.*, 2011, **57**, 749-764.
34. C. A. Flores, E. A. Flores, E. Hernandez, L. V. Castro, A. Garcia, F. Alvarez and F. S. Vazquez, *J. Mol. Liq.*, 2014, **196**, 249-257.
35. B. Cao, J. Du, S. Liu, X. Zhu, X. Sun, H. Sun and H. Fu, *RSC. Adv.*, 2016, **6**, 10462-10470.
36. J. Foster and F. Weinhold, *J. Am. Chem. Soc.*, 1980, **102**, 7211-7218.
37. A. E. Reed, L. A. Curtiss and F. Weinhold, *Chem. Rev.* , 1988, **88**, 899-926.
38. M. Frisch, G. Trucks, H. B. Schlegel, G. Scuseria, M. Robb, J. Cheeseman, G. Scalmani, V. Barone, B. Mennucci and G. Petersson, *Wallingford, CT*, 2009, **19**, 227-238.
39. G. Padiyar and T. Seshadri, *Nucleos. Nucleot. Nucl.*, 1996, **15**, 857-865.
40. M. Novak, C. Foroutan-Nejad and R. Marek, *PCCP.*, 2015, **17**, 6440-6450.
41. Y.-X. Lu, J.-W. Zou, Y.-H. Wang and Q.-S. Yu, *J. Mol. Struct. THEOCHEM.*, 2006, **767**, 139-142.
42. W. Wang, B. Ji and Y. Zhang, *J. Phys. Chem. A*, 2009, **113**, 8132-8135.
43. O. V. Shishkin, I. V. Omelchenko, A. L. Kalyuzhny and B. V. Paponov, *Struct. Chem.*, 2010, **21**, 1005-1011.

Graphical abstract

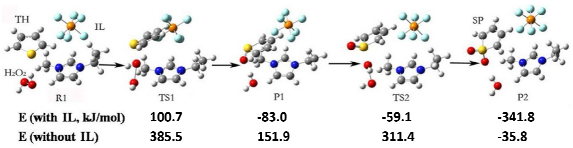

The oxidation of TH to SP by H_2O_2 with the assistance of IL experiences two steps via two transition states.